ELSEVIER

Biophysical Chemistry 97 (2002) 17–27

Biophysical Chemistry

www.elsevier.com/locate/bpc

Kinetics of iron release from pig spleen ferritin with bare platinum electrode reduction

H.Q. Huang[a,b,*], Q.M. Lin[b,c], T.L. Wang[a,d]

[a]*MOE of Key Laboratory for Cell Biology and Tumor Cell Engineering, School of Life Sciences, Xiamen University, Xiamen 361005, PR China*

[b]*State Key Laboratory for Physical Chemistry of Solid Surfaces, Xiamen University, Xiamen 361005, PR China*

[c]*MOE of Key Laboratory for Marian and Environmental Sciences, Xiamen University, Xiamen, 361005, PR China*

[d]*Institute of Molecular and Cell Biology, National University of Singapore, 117690, Singapore, Singapore*

Received 6 November 2001; received in revised form 4 January 2002; accepted 4 January 2002

Abstract

Several anaerobic electrochemical cells were employed to study the kinetics of iron release from pig spleen ferritin (PSF) at a bare platinum electrode. Controlled potential microcoulometry (CPM) is the principal technology used to investigate the kinetics in the absence of a mediator. A kinetic study of iron release by microcoulometry has revealed that ferritin undergoes direct electron transfer at the electrode in the absence of a mediator, indicating that ferritin is an electroactive protein. Several experiments failed to show that α′α-bipyridyl has the capacity to reduce hydrolyzed Fe^{3+} within the ferritin core after it has been reduced by the electrode at −600 mV vs. NHE in the absence of mediator. PSF is known to bind heme to generate a hemeoprotein, named pig spleen hemeoferritin (PSF_{ho}). The rate of iron release is accelerated by the heme binding to PSF_{ho} without the need for small mediators. Under similar conditions, two kinetic processes for iron release from PSF and bacterial ferritin of *Azoaobacter vinelandii* (AvBF) were studied and both fit a zero-order law. In addition, the rate of iron release in PSF can be accelerated two-fold by a specific reduction system consisting of ascorbic acid (AA) and the bare platinum electrode at −600 mV. However, this kinetic process does not follow zero-, half-, first, or second-order rate laws. A model is proposed to explain a mechanism of direct electron transfer between ferritin and the electrode is derived to describe the kinetics of iron release.

Keywords: Pig spleen ferritin; Bioelectrochemical cells; Heme and phosphate role; Platinum electrode; Electron transfer; Kinetics of iron release

Abbreviations: PSF, pig spleen ferritin; AvBF, bacterial ferritin of *Azotobacter vinelandii*; AA, ascorbic acid; HSF, horse spleen ferritin; CPM, controlled potential microcoulometry; MV, methyl viologen; ESD, electrochemical synthesis detector; MPA, 3-mercaptopropionic acid; ETH, electron-tunnel-heme; PSF_{ho}, heme binding to PSF to generate a hemeoprotein; PSF_p, extra phosphate and PSF are mixed to establish a new 1:1 ratio of Pi/Fe^{3+}; ETP, electron transfer pathway; MALDI-TOF, matrix-assisted laser desorption/ionization–time of flight mass spectrometry

*Corresponding author. Tel.: +86-0592-2186392; fax: +86-0592-2186630.

E-mail address: hqhuang@jingxian.xmu.edu.cn (H.Q. Huang).

0301-4622/02/$ - see front matter
PII: S0301-4622(02)00007-8

1. Introduction

Iron is an essential metallic element for the growth and well-being of almost all living organisms [1–6]. Ferritin is a naturally occurring protein with complex structure, consisting of a 24-subunit protein shell used to store iron oxides and phosphate molecules in a mineral core. A single ferritin complex can store up to 4500 hydrolyzed Fe^{3+} oxides [1], although, on average, 1800–2300 Fe^{3+} per molecule of ferritin is observed [6–12]. In mammals, ferritin consists of a protein shell with 24 highly symmetrical subunits and an overall diameter of 120 Å [12]. The iron core of mammalian ferritin is approximately 55–70 Å in diameter, is located at the shell center, and has been observed using electron microscopy [1,13]. As previously mentioned, two basic physiological functions of the ferritin in vivo are to store surplus iron from the extracellular medium and to release it to the intracellular contents [1,7].

In electrochemical studies of ferritin previously described by Watt et al. [14], two reduction potentials of −475 mV for heme reduction from AvBF and −420 mV for its iron core reduction were determined by CPM equipped with the platinum electrode in the presence of methyl viologen (MV). Under similar conditions, the midpoint potential of HSF, initially measured to be −205 mV, shifts negative at a rate of −115 mV/pH, as previously described by Huang et al. [15]. In addition, direct electron transfer from HSF was observed at a gold electrode modified with 3-mercaptopropionic acid (MPA) [16]. From these experimental results, it is inferred that MV and MPA play an important role in transferring the electrons from the electrode to the ferritin for iron release. Conversely, it has been shown that some specific proteins in nature, such as the MoFe protein of nitrogenase [17], cytochrome *c* [18], ferredoxins, heme-containing enzymes [19] and blue Cu protein [20] can also be directly reduced at the metal electrode without mediators or other small organic molecules. Moreover, similar electrochemical behavior of both HSF at gold electrodes and AvBF at platinum electrodes has been directly observed in the absence of a mediator [21–23]. These processes indicate that both proteins, like cytochrome *c*, show electroactive characterizations. In bioelectrochemical studies, the process of direct electron transfer between proteins occurs with increasingly complex systems, including multi-centered enzymes. Also, the electrochemical response of active sites is being used more often as a useful diagnostic signal, in many ways analogous to that provided by various spectroscopic methods [10,17–20].

In the visible range, HSF and PSF show featureless absorbance peaks. In contrast, AvBF shows three peaks at 417, 526, and 557 nm due to the heme component in its protein shell, which shows three characteristic absorbance peaks in the visible range [24–26]. Recent studies show that HSF binds heme to generate a hemeoprotein (HSF_h) [26]. One of the roles of binding heme has been suggested to be the accelerated rate of iron release [26]. Recent experiments suggest that Fe^{3+}, located electron-tunnel-heme (ETH) in AvBF, can be replaced by Co^{2+} to form another structure of ETH-Co^{2+} after the ferritin is treated by cobalt chlorides, named $AvBF_{co}$ [23]. Interestingly, the rate of iron release in $AvBF_{co}$ is decelerated, indicating that this ETH-Co^{2+} structure has lost the capacity to pick up electrons from the electrode for iron release in the absence of mediator [23].

In kinetic studies, the processes of iron release and deposition in mammalian and bacterial ferritins has been described in detail by the stopped-flow technique or spectrophotometry [9,24,27–29]. However, most of the present knowledge on the mechanism(s) of iron release has resulted from extensive studies on readily obtainable mammalian ferritins in vitro [30,31]. Earlier studies showed the rate of iron release depends strongly on the Fe^{3+}/P_i ratio on the surface of the ferritin core [32]. However, recent studies show that three kinetic parameters for iron release, the rate, the biphasic behavior and the mixed orders, are strongly dependent on the regulation speed of the ferritin shell itself, rather than the composition of the core structure [11,32]. Moreover, it has been found that the rate of iron release can be accelerated 10-fold by using the mixed reducers $Na_2S_2O_4$ and reduced MV [9], or two-fold by utilizing another mixture with both $Na_2S_2O_4$ and ascorbic acid [24]. Kinetic characteristic analyses of both mixed reducer sys-

tems shows that the accelerating rate could not change the original pathway with mixed-orders for complete iron release over a simple it with first-order or second-order. This observation suggests that the mixed-orders are controlled by the regulation capacity of protein shell itself, rather than increasing the rate of iron release [11,23].

In this report, a kinetic study for iron release from PSF is performed using CPM with a bare platinum electrode at −600 mV vs. NHE in the absence of a mediator. As shown with AvBF [22], it is logical that PSF might also have a structure with an electron heme-free pathway on the protein shell, and that the heme binding to PSF_{ho} generates a structure of electron transfer pathway (ETP) that accelerates the rate of iron release. The heme functions in PSF_{ho} are similar to that in AvBF.

2. Materials and methods

2.1. Materials

Strain OP of *A. vinelandii* was a gift from The Center for Study of Nitrogen Fixation, College of Agricultural and Life Science, University of Wisconsin–Madison. Most chemicals, including α′α-dipyridyl, AA and MV were from Sigma and of analytical purity.

2.2. Methods

2.2.1. Bacterial culture and AvBF preparation

The strain was cultured in Burk medium-free nitrogen and supplied with sucrose as the sole carbon and energy source. The whole cells were harvested by centrifugation ($6\times1000\times g$) at the end of the logarithmic growth. Crude AvBF was isolated by the method of Bulen et al. AvBF [33] was further purified on a DEAE-cellulose column (4×14 cm) by Burgess [34]. The purified AvBF showed a single peak using high-performance liquid chromatography (HPLC) or a single band with polyacrylamide gel electrophoresis (PAGE).

2.2.2. PSF preparation and purification

A 1:2 weight ratio of pig spleen to distilled water at pH 7.0 was mixed after removal of the lymph and fat tissue, and then homogenated by a homogenizer (6000 rev./min). The homogenate solution was heated to 70–75 °C in a water thermostat for 8 min to denature most proteins (except for PSF). The solution was filtered with an eight-layer gauze, and a red brown filtrate was obtained after cooling. The filtrate was centrifuged at $5\times1000\times g$ for 45 min, the supernatant collected and then the sediment discarded. Finally, the supernatant was further separated on a DEAE-cellulose column (2×24 cm) previously equilibrated with 0.025 M Tris–HCl (pH 7.0)/0.15 M NaCl. The purified PSF exhibited a single band with gel electrophoresis.

2.2.3. Element and protein concentration analysis

Total Fe^{3+}/ferritin was measured using α′α-dipyridyl by spectrophotometry at 520 nm as previously described by Harrison et al. [1]. The phosphate content within the ferritin core was determined by normal Cooper method [35]. Protein concentration measurements were carried out by the Lowry procedure using bovine serum albumin of 98% purity as a protein standard.

2.2.4. Electrode system of the cell and measurement of ferritin spectrum

The electrochemical cells employed to study iron release of ferritin consist of an anaerobic vessel and three electrodes. The electrodes in cells are described as follows: (1) a radiometer fiber-tipped saturated (KCl) calomel electrode (SCE) as the reference electrode; (2) an isolated fine platinum wire as the counter electrode (anode); and (3) a mercury or platinum electrode as the working electrode. Fig. 1 shows an anaerobic electrochemical cell equipped with a platinum electrode. In this cell, compared to normal mercury electrolytic cell, a distinguishable part shows a large working electrode of round platinum (18×56 mm) instead of the mercury electrode. In addition, the SCE and counter electrode are easily removed to add the electrolyte to maintain constant potentials for the desired time.

Fig. 2 shows another electrochemical cell equipped with an air filter and a shut-off valve. This apparatus was used to oxidize Fe^{2+} within the ferritin core into Fe^{3+} by controlling different O_2 concentrations. The O_2 concentration for ferri-

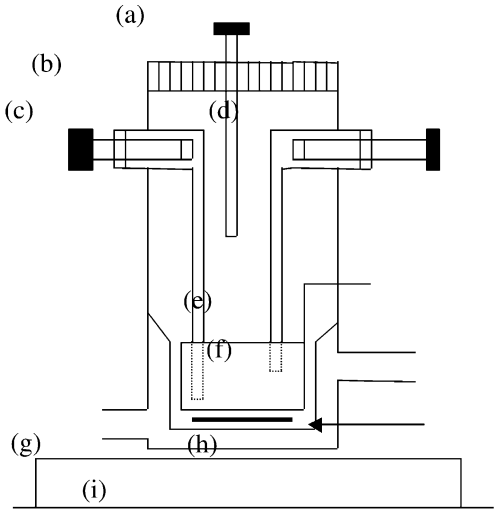

Fig. 1. An anaerobic electrochemical cell equipped with a platinum electrode as the cathode. Distances of 0.2, 0.4 and 1.3 cm are maintained between the SCE and the working platinum electrode (cathode), between the working platinum electrode and the counter electrode (anode), and between the SCE and the counter electrode, respectively, before use. (a) Connecting tube for evacuating and flushing; (b) rubber serum stopper; (c) counter electrode; (d) SCE; (e) platinum electrode (cathode); (f) outlet for flowing water; (g) inlet for flowing water; (h) magnetic stirrer bar; and (i) magnetic stirrer.

tin oxidization within the cell shown in Fig. 2 is measured by gas chromatography with a thermal conductively detector and a molecular sieve 5-Å column (Ar). Shown in Fig. 2, a large working electrode (cathode, 10×80 mm) in the cell is employed to increase the collision rate between the ferritin molecules and the electrode. Moreover, in order to increase enzyme catalysis activity in the living cell, this apparatus, shown in Fig. 2, is also placed into a water thermostat–oscillator to obtain a high oscillating rate. A 0.2-ml cuvette equipped with an anaerobic system was then automatically evacuated and flushed with argon at least three times before the samples from the cells is injected. Under anaerobic conditions, the reduced ferritin sample from the cell was quickly placed into a cuvette for spectral measurement, and then replaced in the cell for further reduction of released iron.

2.2.5. Reduced power of α′α-dipyridyl

A solution of 400 μl α′α-dipyridyl and 1.10 ml 0.025 M Tris–HCl/0.15 M NaCl were mixed and placed in the cell shown in Fig. 2. Then, the cell was automatically evacuated and flushed with 99.99% argon to obtain an anaerobic environment. Next, the reduction potential of −600 mV vs. NHE was employed to the cell to reduce the α′α-dipyridyl for 45 min. Then, 1.0 ml of anaerobic PSF was added to the cell to observe the reaction of iron release, which was monitored with the spectrophotometer at 520 nm after the controlled potentials were closed. However, the experimental results showed no observed evidence of iron release from the protein, which means that the α′α-dipyridyl treated by the electrode neither picked up the electrons from the electrode, nor supported them to the core within the protein shell for iron reduction. Clearly, unlike other redox mediators, α′α-dipyridyl hardly shows any power to reduce iron. Using CPM in the absence of a mediator or of other small reductants, it is indicated that a pathway of transferring electrons for iron release can be considered from the electrode to ferritin.

2.2.6. Kinetic measurement of iron release

The cell in Fig. 1 was used to study the kinetics of iron release by the CPM in the absence of a mediator. A solution of 3.0 ml ferritin (3.0 mg/ml) and a 150-μl α′α-dipyridyl were mixed with a magnetic stirrer for 2 min. The mixture was then placed into the anaerobic cell, and reduced by an electrochemical synthesis detector (ESD) equipped with a three-electrode system without the need for

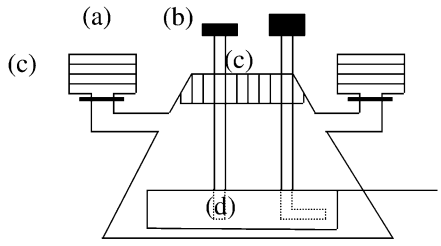

Fig. 2. Diagram of the electrochemical cell designed to produce PSF_h. (a) Counter electrode; (b) SCE; (c) air filter and shut-off valve; and (d) working platinum electrode.

a small mediator. The rate of iron release was measured by a spectrophotometer equipped with a double light system at 520 nm over the desired time period.

2.2.7. Heme binding to PSF

Excess heme chloride (200 μl) in 0.01 M NaOH and 10.0 ml of PSF (3.0 mg protein/ml) were mixed with a stirrer for 20–30 min. The mixture was quickly placed into the cell (Fig. 2) for protein reduction at a potential of −600 mV vs. NHE for 40 min. Next, the reduced mixture was slowly oxidized in air for 60 min with a controlled O_2 pressure (0.21 atm.), and then separated on a Sephadex G-25 column (2×12 cm) for separating dissociating heme and collecting oxidized PSF_h, named PSF_{ho}. Finally, PSF_{ho} spectra were recorded by a double bean spectrophotometer at 30 °C, pH 7.20.

2.2.8. Kinetic studies of iron release with ascorbic acid reduction

A solution of 2.0 ml ferritin (0.5 mg/ml) and a 60-μl α′α-dipyridyl, was placed in a 10-ml calibrated vial fitted with rubber serum stopper. The vessel was then automatically evacuated and flushed with argon at least six times. Next, 300 μl saturated AA was injected into the vessel for quick iron reduction. The vessel was shaken to start a reaction of iron release in the water thermostat, and then the sample solution was quickly injected into the anaerobic cuvette for kinetic measurement of iron release. The rate of this reaction was determined spectrophotometrically at 520 nm according to the desired reaction time.

2.2.9. Kinetic studies of iron release with the electrode and ascorbic acid reduction simultaneously

A solution of 3.0 ml ferritin and 80 μl α′α-dipyridyl, were mixed with a stirrer, then the mixture was placed in the cell shown in Fig. 1. Next, the cell was evacuated and flushed with the appropriate argon gas as using an automatic instrument five times. Next, 0.30 ml of a saturated AA solution was injected into the cell quickly. The mixture in the cell was reduced by the special reduction system consisting of an electrode at −600 mV vs. NHE and AA. The rate of iron release was measured by a spectrophotometer at 520 nm according to the desired reaction time.

2.2.10. Effect of extra phosphate on iron release

A 10.0-ml sample of PSF having a 1:8 ratio of iron to phosphate was prepared, and then extra phosphate was added to the sample solution to form a new ratio of 1:1 in the reaction medium, which was called PSF_P. The mixture was then placed into the anaerobic cell (Fig. 1) containing α′α-dipyridyl, and reduced by the electrode at −600 mV. The date of iron release was recorded by at 520 nm as a function of time [11,36].

3. Results

3.1. Electrochemical behavior of the ferritins at the mercury electrode

During voltammetry with scan potentials ranging from +200 to −600 mV vs. NHE at scan rate 5 mV/s, pH 7.25 at 30 °C in the absence of a mediator, the experimental results show that the reduction current for both PSF and AvBF as measured on the mercury electrode, respectively, appear sluggish on the electrode. Of course, the experimental result shows that no evidence of iron release from the ferritins was observed. For these reasons, we have examined a different electrode material.

3.2. Electrochemical behavior of PSF on the platinum electrode

Using CPM and the cell shown in Fig. 1, it appears that similar to AvBF, PSF undergoes a reductive reaction at the electrode without a mediator (Fig. 3). The straight line in Fig. 3a shows an average rate 2.3 Fe^{3+}/min/PSF in 460 min. However, this rate is lower than the rate of 10.5 Fe^{3+}/min/AvBF in AvBF as recently described [22]. In similar studies, it was observed that only 50% (1060 Fe^{3+}/PSF) of original Fe^{3+} (2120 Fe^{3+}/PSF) in PSF is only released in 460 min. The results suggest that there are two populations of iron present. The first is really lost, but the remaining Fe^{3+} within the protein shell is sluggish

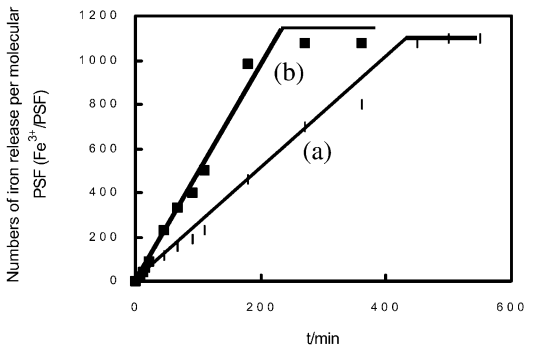

Fig. 3. Kinetics of iron release from PSF at controlling potential of −600 mV vs. NHE. The kinetics of iron release for both curves (a,b) are defined as zero-order reactions. In curve (a), the rate constant K is 2.3 Fe^{3+} min^{-1} PSF^{-1} and the half-life time $t_{1/2}$ is 225 min. In curve (b), after the addition of phosphate, the rate constant K_p is 4.8 Fe^{3+} min^{-1} PSF^{-1} and the half-life time $t_{1/2p}$ is 105 min. (a) Spectra of heme chloride in 0.015 M NaOH. (b) Spectra of PSF_h. PSF_h and free-heme in the mixed samples were separated on a Sephadex G-25 column before spectral measurement. (c) Spectra of PSF.

to accept electrons from the electrode without a small mediator.

To study the role of P_i in iron release reaction, extra phosphate and PSF were mixed to establish a new 1:1 ratio of P_i/Fe^{3+} (PSF_p). Using CPM, the rate of iron release is accelerated with increasing phosphate content, giving an average rate of 4.8 $Fe^{3+}/min/PSF_p$ (Fig. 3b). The rate increment in the presence of extra phosphate is two-fold higher than that in PSF, but because similar numbers of iron ions were released from both PSF and PSF_p (Fig. 3a,b), phosphate only increases the rate of half of the iron present. These results suggest that the phosphate binding to the ferritin has the capacity to affect Fe^{3+} stability of only half of iron present within the protein's core.

An important step in understanding the mechanism of phosphate storage from the ferritin was previously described by Watt [37] and Huang [24,36]. These authors show that the extra phosphate could not only be stored by the ferritin in the presence of Fe^{2+} and O_2 (0.21 atm.), but was most likely bound to the three-fold channel of the ferritin shells [24,36]. Phosphate binding to the channel plays a role in inhibiting the rate of iron release while the small molecular reductants such as AA and $Na_2S_2O_4$ were used to reduce Fe^{3+} within the ferritin's core [11]. As illustrated by these reports, one of the basic reaction conditions for carrying out iron reduction and release with these reductants such as $Na_2S_2O_4$ and with the Fe^{2+} chelating agent must pass through the three-channel of the ferritin shell into the iron core [11]. We conclude that the effect of the phosphate binding to the channel on the transfer rate of reduction of Fe^{3+} to Fe^{2+} accelerates the rate of reaction of the Fe^{2+} chelating agent across the protein shell, which in turn causes the rate of iron release to decrease. Conversely, using CPM and in the presence of Fe^{2+} and O_2, the phosphate binding to the ferritin shell takes advantage of picking up the electrons from the electrode so that the rate of iron release increases. It is proposed that the phosphate not only binds to the ETP across the protein shell, but also participates in picking up the electrons from the electrode and transferring the electrons for iron release, and that no other reductants share the three-fold channel as a route with the Fe^{2+} chelating agent during iron release with CMP technology in the absence of a mediator, which results in the rate of iron release increasing greatly [22,27].

3.3. Electrochemical behavior of PSF_{ho} and AvBF

Fig. 4c shows that PSF exhibits a featureless absorbance peak in the visible spectra range from 350 to 600 nm and that its absorbance intensity decreases as the wavelength increases into the red (bottom spectrum). Moreover, heme chloride (Fig. 4a) has three absorbance peaks at 555 (α), 525 (β), and 414 (Soret band) nm, indicating that the heme forms three peaks in the visible range. Unlike PSF, PSF_{ho} (Fig. 4b) also exhibits three absorbance peaks at 555 (α), 525 (β), and 414 (Soret band) nm, confirming that the heme not only binds to the PSF, but also generates PSF_{ho}, resulting in ferritin, which also shows the three characteristics peaks from heme.

Using the CPM, both experimental results in Fig. 5 show two kinetic studies of iron ions released from both PSF_{ho} and AvBF against time, giving two straight lines. In Fig. 5a, the rate constant K_{avbf} of complete iron release from AvBF

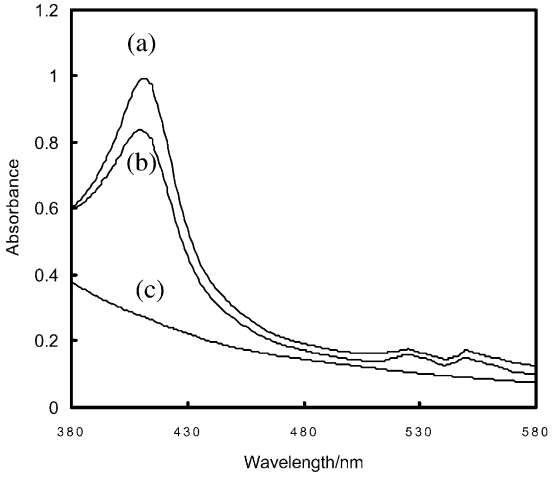

Fig. 4. Electronic spectra of PSF and PSF_{ho}. The results in curve A show the kinetics for complete iron release from AvBF at a controlled potential of −600 mV vs. NHE in the absence of mediator, which is defined as a zero-order reaction. Compete iron within the ferritin's core is directly released by the potential without chemical reductant such as dithioinite aid. The rate constant K_{avbf} is 10.5 Fe^{3+} min^{-1} $AvBF^{-1}$ and its half-life time $t_{1/2}$ is 91.5 min. The results in Curve (b) show the kinetics of iron release from PSF_{ho} at a controlled potential of −600 mV vs. NHE in the absence of a mediator, which is defined as a zero-order reaction. Half of the original iron ion concentration within the PSF_{ho} core is released by the potential without chemical reductant such as MV aid. The rate constant K_{psfho} is 4.2 Fe^{3+} min^{-1} PSF_{ho}^{-1}.

is 10.7 Fe^{3+}/min/AvBF, for which the kinetic process is known to fit the zero-order law as long as the constant rate (K_{avbf}) is observed. In a similar study, Fig. 6b shows that 50% (1050 ± 20 Fe^{3+}/PSF_{ho}) of the original Fe^{3+} within the protein core is also released. A constant rate (K_{psfh}) of 4.2 Fe^{3+}/min/PSF is obtained, meaning that this kinetic process fits the zero-order law. Comparing both results in Figs. 3 and 5, it is noted that the rate is accelerated two-fold by the heme in PSF_{ho}, indicating that the heme played an important role in accelerating the rate of electron transfer from the electrode to the protein. Interestingly, using CPM, similar numbers (1050 ± 20 Fe^{3+}/PSF) of iron release among PSF, PSF_p and PSF_{ho} are still observed. These results indicated that the heme and extra phosphate bind to the surface of the protein shell rather than to the iron core because

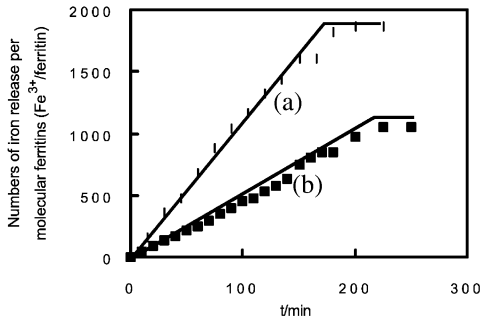

Fig. 5. Kinetics of iron release from PSF_{ho} and AvBF at a controlling potential of −600 mV vs. NHE. Curve (a) (▲): the kinetic curve of complete iron release from PSF_{ho} with a mixed reduction system consisted of ascorbic acid and the electrode at a controlled potential of −600 mV vs. NHE simultaneously; average rate of iron release 52.0 Fe^{3+} PSF_{ho}^{-1} min^{-1} is obtained. Curve (b) (■): kinetic curve for complete iron release from PSF_{ho} with an ascorbic acid reduction; an average rate 32.0 Fe^{3+} PSF_h^{-1} min^{-1} is observed. Curve (c) (▼): the kinetic curve for complete iron release from PSF with an ascorbic acid reduction; an average rate of 31.0 Fe^{3+} PSF^{-1} min^{-1} is obtained.

similar numbers of iron released among PSF, PSF_p and PSF_{ho} can clearly be observed. Evidently, the heme in PSF_{ho} and the phosphate in PSF_p play

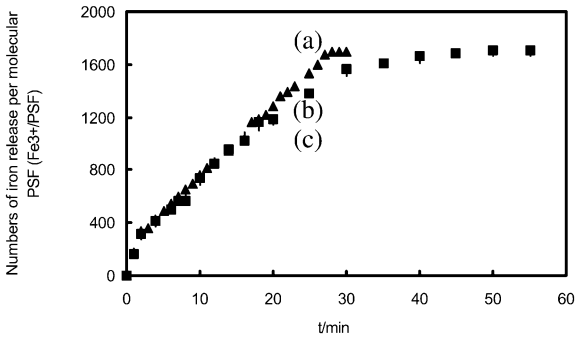

Fig. 6. Kinetics of complete iron release from PSF. Curve (a) (▲): the kinetic curve of complete iron release from PSF_{ho} with a mixed reduction system consisted of ascorbic acid and the electrode at controlled potential of −600 mV vs. NHE simultaneously; average rate of iron release 52.0 Fe^{3+} PSF_{ho}^{-1} min^{-1} is obtained. Curve (b) (■): kinetic curve for complete iron release from PSF_{ho} with an ascorbic acid reduction; an average rate of 32.0 Fe^{3+} PSF_h^{-1} min^{-1} is observed. Curve (c) (▼): the kinetic curve for complete iron release from PSF with an ascorbic acid reduction; an average rate of 31.0 Fe^{3+} PSF^{-1} min^{-1} is obtained.

roles in increasing the amount of iron released hardly while the Fe^{3+} within the ferritin's core is reduced by the electrode at −600 mV. However, both roles are suggested to improve the ability of the ferritin for picking up the electrons from the electrode or accelerating the rate of electron transfer across the protein shell in which results an increase of the rate of iron release. The structure analysis indicated that high ratio of phosphate to iron (1:1.2) of the iron core from AvBF [27] and its heme structure across the protein shell were observed. According to this structure, we reasoned that a complete iron core with high ratio of phosphate to iron can pick up the electrons from ETP for iron release in the absence of mediator, which causes a complete iron core released by the electrode reduction at high rate. However, another structure analysis indicated that the core has a low ratio of phosphate to iron (1:13) structure from PSF_{ho} [11], and that the heme binds only to the surface of the protein shell are observed, which causes only half of the iron core to be able to pick up the reduction electrons came from the ETP for iron release. Clearly, the phosphate content within the protein shell plays an important role in assisting the iron to accept the electrons from the ETP for it reduction.

3.4. Kinetics of iron release from PSF

AA is a biological electron donor and has a midpoint potential of $E^{o}_{1/2} = -14$ mV vs. NHE [38]. The AA potential is higher than that both AvBF ($E^{o}_{1/2} = -125$, −310 and −370 mV) [22] and HSF ($E^{o}_{1/2} = -480$ mV) [14]. In appearance, it is impossible for the Fe^{3+} component within the ferritin core to be directly reduced with AA according to both potential differences. However, a study of iron binding to ferritin that can catalyze ascorbate oxidation was done by Roginsky et al. [39], meaning that Fe^{3+} within the ferritin shell can be directly reduced by AA. The mechanism by which AA not only binds directly to the ferritin shell, but also causes its conformation change as well as greatly decrease its reduction potential, which results the protein shell and the iron core being reduced by AA, has been described in detail by Huang [24,40]. According to the results shown in Fig. 6c, it is can be clearly seen that a kinetic process of complete iron release from the PSF is easily completed with AA under anaerobic conditions in 60 min, giving an average rate of 31.0 Fe^{3+}/min/PSF. It is observed that the rate increment shown in Fig. 6c is 13-fold higher than that of the protein (2.3 Fe^{3+}/min/PSF) with the electrode reduction in Fig. 3a.

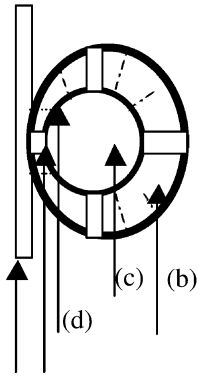

Fig. 7. A model of electron transfer between the electrode and ferritin in the absence of a mediator. (a): The platinum electrode; (b) ferritin shell; (c) iron core; (d) the electron tunnel; and (e) the three-fold channel.

Moreover, under similar conditions, the kinetics of iron release from PSF_{ho} are also measured with AA reductant (Fig. 6b), showing an average rate 32.0 Fe^{3+}/min/PSF_{ho} at pH 7.25, 30 °C. Evidently, the close rate of iron release by both PSF and PSF_{ho} is observed (Fig. 7b,c) while Fe^{3+} within the ferritin's core is reduced by AA, indicating that the heme in the latter protein plays a minor role in accelerating the rate. However, the rate of iron release using AA as a reductant is faster than the rate used at the electrode at −600 mV. This behavior is significant, as it indicates that the pathway of electron transfer that AA utilizes might differ from that which the electrode utilizes. These findings further support the viewpoint that there are multiple pathways of electron transfer in PSF, which suggest that the pathway used by AA differs from that used by the electrode. Interestingly, neither of the curves shown in Fig. 6b,c fits zero-, first-, or second-order rate laws because none have a straight line plot of rate of iron release as a function of reaction time. Clearly, these behaviors

demonstrate that the complex kinetic process for complete iron release both PSF and PSF_h are formed with AA only, not by the heme in PSF_{ho}.

The experimental results shown in Fig. 6a show that the rate for complete iron release from PSF_{ho} is accelerated by the reduction system consisting of AA and the electrode, given an average rate of 52.0 $Fe^{3+}/min/PSF_{ho}$. However, it is surprising that this kinetic curve in Fig. 6a still fits neither zero-, first- nor second -orders laws, though the rate increases. These experimental results suggest that the complex kinetic process for the complete iron release was formed by AA, but not by the electrode. The kinds of electron transfer pathway across the protein shell used by AA might differ from that used by the electrode. However, both pathways would be selected and used by AA and the electrode at a similar time, which results in the rate of iron release being accelerated.

4. Discussion

Mercury is a bactericide that can cause the proteins in nature to partially be denatured. Ferritin's shell, including the ETH or ETP structures, might easily be destroyed after mixing with liquid mercury. As a result, it is suggested that the reason that ferritin exhibited no electroactivity on the mercury electrode [41] is because its ETH had been destroyed by the liquid mercury in advance, resulting in the ferritin losing its capacity to pick up electrons from the electrode.

Like AvBF, a process of iron reduction shown in Figs. 2 and 5 between the PSF and the platinum electrode is observed. These electrochemical behaviors in PSF and HSF [21] are indicative that both proteins are electroactive. However, one important issue in ferritin research is whether the electrode has the capacity, while in direct contact with the protein, to transfer electron to the iron within the protein's core to supply the electrons for iron release. Clearly, the electrode size shown in Figs. 1 and 7 appears to be too large to penetrate the three-fold channel of the protein shell into the core to carry out an iron reaction. A pathway for transferring electrons between the ferritin's core and the electrode should depend on the ETP across the protein shell. The present study addresses three pathways described in the ferritin, which are described as follows: (1) a three fold-channel having a nominal diameter of 7–9 Å constitutes a possible pathway through which iron and other molecular species gain access to the ferritin core. (2) A four-fold channel has been shown at the intersections of four peptide subunits that might act as an electron pathway for iron reduction. (3) An ETH across the protein shell has been indicated to pick up the electron from the electrode and to transfer them to the ferritin core for iron release [22]. From these observations and analysis, it is determined that there is ETP in PSF or ETH in AvBF, where the reaction of iron release occurs on the bare electrode. However, only half of the iron can be reduced, the heme and phosphate binding to PSF_{ho} and PSF_p were shown to improve the capacity of electron transfer between the electrode and ferritin, which causes the rates of iron release for both proteins to be accelerated.

From the results reported here, we propose a model for electron transfer between the ferritin and the electrode. First, an electrode with low potential produces a strong capacity for absorbing ferritin to the electrode [21]. Secondly, the ferritin is easily absorbed on the electrode to produce a distorted protein while colliding with the electrode by diffusion (Fig. 7). Finally, the ferritin undergoes a process of iron reduction after the electrons coming from the electrode are picked up by the electron tunnel across the protein shell. To obtain information on how the potential affects the rate of iron release, liver ferritin of *Dasyatis akajei* was incubated with different potential ranging from -200 to -500 mV and the experimental results reveal that the rate of iron release depended strongly on the potential [40]. Moreover, matrix-assisted laser desorption/ ionization-time of flight (MALDI-TOF) mass spectrometer has been employed to study charge distribution on the surface of ferritin shell, which indicates that there are positive charges range with high density on the surface of the shell which results in the protein was attracted to the electrode with negative potential [41]. These novel behaviors indicate that the distorted protein formed by the electrode plays an important role in accelerating the electron transfer from the electrode to the ferritin's core. It is inferred that the possi-

bility of electron transfer between the electrode and the protein occurred by the electron pathway across the shell of distorted ferritin.

As described by Jacobs et al. [42], the experimental results using Mossbauer spectroscopy have indicated that phosphate on the mineral iron core plays an important role in catalyzing the internal electron transfer reaction from Fe^{2+} to Fe^{3+}. If this is the case, most Fe^{3+} in the AvBF core can utilize the electrons from the electrode for iron release because it has a higher ratio of phosphate to iron (1:1.2) than that in PSF (1:8) [11,15]. An iron structure with a 1:3 ratio of Fe^{3+}/P_i is found on the surface of the core from HSF, with a ratio higher than that (1:16) on the inside of the iron core, as previously described by Huang et al. [15]. Evidently, using the CPM, Fe^{3+} composition on the surface of the PSF core can still utilize the electron coming from the electrode because of its high phosphate content. However, the Fe^{3+} that remains within the protein core loses this capacity because of insufficient phosphate.

Acknowledgments

This project is supported by the State Natural Science Foundation of China (No. 49876027) and by the Foundation for University Key Teacher by the Ministry of Education in China and the Natural Science Foundation of Xiamen State in China (2001-06), awarded to H.Q. Huang. The authors wishes to thank graduate students Z.Q. Xiao for their help in the HPLC and EC analysis of the ferritins, and B. Kong, T.M. Caoand N.C. Huang for their help for supplying the ferririn samples. We also thank Drs Y.S. Zhang and A.B. Hummon for many helpful discussions and proofreading.

References

[1] P.M. Harrison, I.G. Hoy, I.G. Macara, R.J. Hoare, Ferritin iron uptake and release, Biochem. J. 143 (1974) 445–447.

[2] J.L. Johson, C.D. Norcross, P. Arosio, R.B. Frankel, G.D. Watt, Redox reactivity of animal apoferritins and apoheteropolymers assembled from recombinant heavy and light human chain ferritins, Biochemistry 38 (1999) 4089–4096.

[3] E.C. Theil, Ferritin: structure, gene regulation, and cellular function in animals, plants, and microorganisms, Ann. Rev. Biochem. 56 (1987) 289–315.

[4] H.Q. Huang, Q.M. Lin, Z.B. Lou, Construction of a ferritin reactor: an efficient means for trapping various heavy metal ions in flowing seawater, J. Protein. Chem. 19 (2000) 441–447.

[5] L.J. Johnson, M. Cannon, R.K. Watt, R.B. Frankel, G.D. Watt, Forming the phosphate layer in reconstituted horse spleen ferritin and role of phosphate in promoting core surface reactions, Biochemistry 38 (1999) 6706–6713.

[6] L.J. Johnson, D.C. Norcross, P. Arpsio, R.B. Frankel, G.D. Watt, Redox reactivity of apoferritins and apoheteropolymers assembled from recombinant heavy and light human chain ferritins, Biochemistry 38 (1999) 4089–4096.

[7] E.C. Theil, H. Takagi, G.W. Small, L. He, A.R. Tipton, The ferritin iron entry and exit problem, Inorganica Chim. Acta 297 (2000) 242–251.

[8] J.P. Laulhere, A.M. Laboure, O.V. Wuytswinkel, J. Gagnon, L.F. Briat, Purification characterization and function of baterioferritin from the *Cyanobacterium synechocystis* P.C.C. 6083, Biochem. J. 281 (1992) 785–793.

[9] T.D. Richards, K.R. Pitt, G.D. Watt, A kinetics study of iron release from *Azotobacter vinelandii* bacterial ferritin, J. Inorg. Biochem. 61 (1996) 1–13.

[10] H.Q. Huang, L.S. Xu, F.Z. Zhang, et al., H_2-uptake activity, spectra, reduction potentials, and kinetics of iron release on the surface of iron core from *Azotobacter vinelandii* bacterial ferritin, J. Protein Chem. 17 (1998) 45–53.

[11] H.Q. Huang, Q.M. Lin, B. Kong, et al., Role of phosphate and kinetic characteristics of complete iron release from native pig spleen ferritin-Fe, J. Protein Chem. 18 (1999) 497–504.

[12] G.C. Ford, P.M. Harrison, D.W. Rice, et al., Ferritin: design and formation of an iron-storage molecule, Philos. Trans. Roy. Soc. London B 304 (1984) 551–565.

[13] Z.Q. Xiao, Ph. D. thesis, Xiamen University, China, 2000.

[14] G.D. Watt, R.B. Frankel, G.C. Papaefthymiou, K. Spartalian, E.I. Stiefel, Redox properties and Mossbauer spectroscopy of *Azotobacter vinelandii* bacterioferritin, Biochemistry 25 (1986) 4330–4336.

[15] H.Q. Huang, R.K. Watt, R.B. Frankel, G.D. Watt, The properties of the surface of iron core from horse spleen ferritin, J. Xiamen Univ. 32 (1993) 628–633.

[16] T.D. Martin, S.A. Monheit, R.J. Niichel, S.C. Peterson, C.H. Campbell, D.C. Zapien, Electron transfer of horse spleen ferritin at gold electrode modified by self-assembled monolayers, J. Electroanal. Chem. 420 (1997) 279–290.

[17] Y.C. Feng, H.Q. Huang, D. Zeng, Studies on the properties of nitrogenase components by cyclic voltametry, J. Xiamen Univ. 26 (1987) 753–755.

[18] T. Sagara, S. Nakajima, H. Akutusu, Y. Niki, Heterogenous electron transfer rate measurement of cytochrome c_3 at mercury electrode, J. Electrochem. Chem. 279 (1991) 271–282.
[19] L. Gorton, A. Lindgren, T. Larrsson, F.D. Munteanu, T. Ruzgas, I. Gazavyan, Direct electron transfer between heme-containing enzymes and electrodes as basis for third generations biosensors, Anal. Chim. Acta. 400 (1999) 91–108.
[20] F.A. Armstrong, G.S. Wilson, Recent developments in Faradaic bioelectrochemistry, Electrochim. Acta 45 (2000) 2623–2645.
[21] D.C. Zapien, M.A. Johnson, Direct electron transfer of ferritin adsorbed at bare gold electrode, J. Electroanal. Chem. 494 (2000) 114–120.
[22] H.Q. Huang, F.Z. Zhang, L.S. Xu, Q.M. Lin, J.W. Huang, D. Zeng, Spectrochemical investigation of *Azotobacter vinelandii* bacterial ferritin, Bioelectrochem. Bioenerg 44 (1998) 301–307.
[23] H.Q. Huang, Q.M. Lin, F.Z. Zhang, C.H. Chen, X. Chen, Z. Chen, Studies on the heme and H_2-uptake reaction from *Azotobacter vinelandii* bacterial ferritin, Bioelectrochem. Bioenerg. 48 (1990) 87–93.
[24] H.Q. Huang, Q.M. Lin, F.Z. Zhang, C. Zhong, Z.B. Lou, L.S. Xu, Studies on characteristics of electron tunnel and pathway of iron release from pig spleen ferritin, Chin. J. Biochem. Mol. Biol. 15 (1999) 10–15.
[25] H.Q. Huang, Q.M. Lin, N. Wu, X.S. Li, Studies on capacity of electron transfer from fish liver ferritin with electrochemical technology, Acta Biophys. SINICA 16 (2000) 457–465.
[26] F.H.A. Kadir, F.K. Al-Massad, G.R. Moore, Haem binding to horse spleen ferritin and its effect on the rate of iron release, Biochem. J. 282 (1992) 867–870.
[27] H.Q. Huang, Q.M. Lin, X. Chen, Z. Chen, L.S. Xu, F.Z. Zhang, Studies on redox characteristics and electrode activity of bacterial ferritin, Acta Biophys. Sinica 15 (1999) 158–165.
[28] T. Jones, R. Spencer, C. Walsh, Mechanism and kinetics of iron release from ferritin by dihydroflavins and dihydroflavin analogues, Biochemistry 17 (1978) 4011–4017.
[29] N. Imai, Y. Umezawa, Y. Arata, S. Fujiwara, An electrochemical study of the iron storage protein, ferritin, Biochim. Biophys. Acta 626 (1980) 501–506.
[30] T.G. Hoy, P.M. Harrison, M. Shabbir, I.G. Macara, The release of iron from horse spleen ferritin to 1,10-phenanthroline, Biochem. J. 137 (1974) 67–70.
[31] S.S. Stefanini, E. Chiancone, E. Antonini, Kinetics of iron reduction of ferritin cores and of a low molecular weight hydroxy-iron polymer, Biochim. Biophys. Acta. 542 (1978) 170–175.
[32] F. Funk, J.P. Lenders, R.P. Crichton, W. Schneider, Reductive mobilisation of ferritin iron, Eur. J. Biochm. 152 (1985) 167–172.
[33] W.A. Bulen, R. LeComte, S. Lough, A homoprotein from *Azotobacter* containing non-heme iron: isolation and cryatallization, Biochem. Biophys. Res. Commum. 54 (1973) 1274–1281.
[34] B.K. Burgess, D.B. Jacobs, E.I. Stiefel, Large-scale purification of high activity *Azotobacter vinelandii* nitrogenase, Biochim. Biophys. Acta. 614 (1980) 196–209.
[35] T. Cooper, Tools of Biochemistry, John Wiley & Sons, New York, 1977.
[36] H.Q. Huang, R.K. Watt, R.B. Frankel, G.D. Watt, Role of phosphate in Fe^{2+} binding to horse spleen holoferritin, Biochemistry 32 (1993) 1681–1687.
[37] G.D. Watt, R.B. Frankel, D. Jacobs, H.Q. Huang, G.C. Papaefthymiou, Fe^{2+} and phosphate interactions in bacterial ferritin from *Azotobacter vinelandii*, Biochemistry 31 (1992) 5671–5679.
[38] H.A. Sober, R.A. Harte, Handbook of Biochemistry, The Chemical Rubber Co, Cleveland, OH, 1970.
[39] V.A. Roginsky, T.K. Barsukova, G. Bruchelt, H.B. Stegmann, Iron bound to ferritin catalyzes ascobate oxidation: effects of chelating agents, Biochim. Biophys. Acta 1335 (1997) 33–39.
[40] H.Q. Huang, Q.M. Lin, B.L. Zhou, D.M. Lou, Studies on capacity of picking up electrons on the surface of iron core from fish liver ferritin, Acta Biophys. SINICA 17 (2001) 668–675.
[41] H.Q. Huang, B. Kong, T.M. Cao, Studies on the charge distribution on the surface of ferritin shell by MALDI-TOF MS technology, Acta Biophys. SINICA 18 (2002) 26–33.
[42] D. Jacobs, G.D. Watt, R.B. Frankel, G.C. Papaefthymiou, Fe^{2+} binding and holo mammalian ferritin, Biochemistry 28 (1989) 9216–9221.